arXiv:1402.0948v1 [cond-mat.supr-con] 5 Feb 2014

Chemical Trend of Superconducting Transition Temperature in Hole-doped $CuBO_2$, $CuAlO_2$, $CuGaO_2$ and $CuInO_2$

Akitaka Nakanishi*, Hiroshi Katayama-Yoshida

Department of Materials of Engineering Science, Osaka University, Toyonaka, Osaka 560-8531, Japan

Abstract

We calculated the superconducting transition temperature T_c of hole-doped $CuBO_2$, $CuAlO_2$, $CuGaO_2$ and $CuInO_2$ using first-principles. The calculated T_c are about 50 K for $CuAlO_2$, 10 K for $CuBO_2$ and $CuGaO_2$ and 1 K for $CuInO_2$ at maximum in the optimum hole-doping concentration. The low T_c of $CuInO_2$ is attributed to the weak electron-phonon interaction caused by the low covalency and heavy atomic mass.

Keywords: A. Semiconductors; C. Delafossite structure; D. Electron-phonon interactions; E. Density functional theory

1. Introduction

$CuAlO_2$ has a delafossite structure (Left of Fig. 1) and a two-dimensional electronic structure caused by the natural super-lattices of O-Cu-O dumbbell. Kawazoe *et al.* have found that the $CuAlO_2$ is p-type transparent conducting oxides (TCO) without any intentional doping. [1] Nakanishi *et al.* studied the pressure dependence of the structures [2] and the role of the self-interaction correction in $CuAlO_2$. [3] Transparent p-type conductors such as $CuAlO_2$ are important for the p-n junction of TCO and a realization of high-efficiency photovoltaic solar-cells. First-principles calculations have shown the possibility for high efficiency thermoelectric power application with about 1% hole-doping. [4, 5, 6]

*Tel.: +81-6-6850-6504. Fax: +81-6-6850-6407.
Email address: nakanishi@aquarius.mp.es.osaka-u.ac.jp (Akitaka Nakanishi)

Katayama-Yoshida *et al.* have simulated the Fermi surface of the hole-doped $CuAlO_2$ by shifting the Fermi level rigidly and proposed that the nesting Fermi surface may cause a strong electron-phonon interaction thus a transparent superconductivity for visible light. [7] However, they have not calculated the superconducting transition temperature T_c. In previous study, we calculated the T_c of hole-doped $CuAlO_2$ [8] and found that the T_c increases up to about 50 K due to the strong electron-phonon interaction by the two dimensional flat valence band. The origin of the flat band is the π-band of hybridized O $2p_z$ and Cu $3d_{3z^2-r^2}$ on the frustrated triangular lattice in the two dimensional plane.

It is interesting to see the relation between the T_c and the flatness of the flat band by changing the Cu $3d_{3z^2-r^2}$, Ag $4d_{3z^2-r^2}$ and Au $5d_{3z^2-r^2}$. In the next study, we calculated the T_c of hole-doped delafossite $AgAlO_2$ and $AuAlO_2$. [9] The calculated T_c are about 40 K for $AgAlO_2$ and 3 K for $AuAlO_2$ at maximum in the optimum hole-doping concentration. The low T_c of $AuAlO_2$ is attributed to the weak electron-phonon interaction caused by the low covalency and heavy atomic mass. In this study, we calculated T_c and the electron-phonon interaction versus the chemical trend of hole-doped $CuBO_2$, $CuAlO_2$, $CuGaO_2$ and $CuInO_2$.

2. Calculation Methods

The calculations were performed within the density functional theory [10, 11] with a plane-wave pseudopotential method, as implemented in the Quantum-ESPRESSO code. [12] We employed the Perdew-Wang 91 [13] for $CuBO_2$, $CuAlO_2$ and $CuGaO_2$ and the Perdew-Burke-Ernzerhof [14] for $CuInO_2$ generalized gradient approximation (GGA) exchange-correlation functional and ultra-soft pseudopotentials. [15] For the pseudopotentials, d electrons of transition metals were also included in the valence electrons. In reciprocal lattice space integral calculation, we used $8 \times 8 \times 8$ (electron and phonon) and $32 \times 32 \times 32$ (density of states and average at Fermi level) **k**-point grids in the Monkhorst-Pack grid. [16] The energy cut-off for wave function was 40 Ry and that for charge density was 320 Ry. These **k**-point grids and cut-off energies are fine enough to achieve convergence within 10 mRy/atom in the total energy.

The delafossite structure belongs to the space group $R\bar{3}m$ (No. 166) and is represented by cell parameters a and c, and internal parameter z (Left of Fig. 1). These parameters were optimized by the constant-pressure variable-cell

relaxation using the Parrinello-Rahman method [17] without any symmetry constraints.

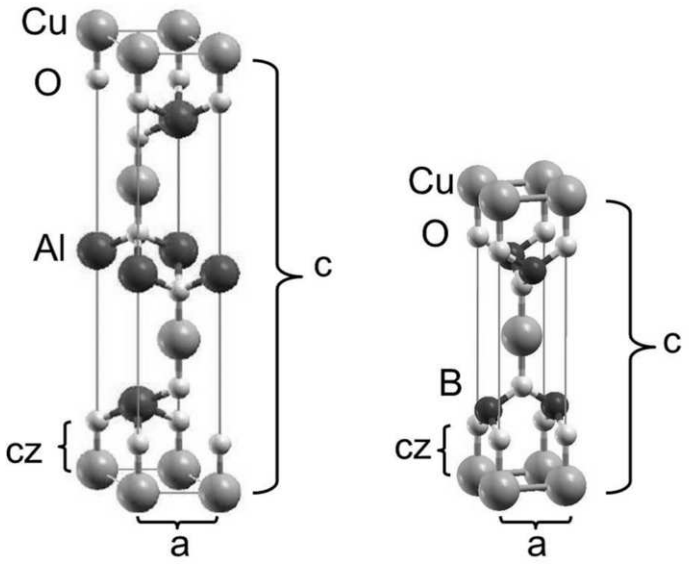

Figure 1: The crystal structure of delafossite $CuAlO_2$ (left) and body-centered tetragonal $CuBO_2$ (right).

As it is difficult for first-principles to exactly deal with doped systems. we had to implement some approximations. Let us take the electron-phonon interaction λ for example. λ is defined as follows:

$$\lambda = \sum_{\nu\mathbf{q}} \frac{2N(\varepsilon_{\rm F}) \sum_{\mathbf{k}} |M^{\nu\mathbf{q}}_{\mathbf{k},\mathbf{k}+\mathbf{q}}|^2 \delta(\varepsilon_{\mathbf{k}} - \varepsilon_{\rm F}) \delta(\varepsilon_{\mathbf{k}+\mathbf{q}} - \varepsilon_{\rm F})}{\omega_{\nu\mathbf{q}} \sum_{\mathbf{k}\mathbf{q}'} \delta(\varepsilon_{\mathbf{k}} - \varepsilon_{\rm F}) \delta(\varepsilon_{\mathbf{k}+\mathbf{q}'} - \varepsilon_{\rm F})}. \quad (1)$$

(1) For the non-doped systems, we calculated the dynamical matrix, the phonon frequency $\omega_{\nu\mathbf{q}}$ and the electron-phonon matrix $M^{\nu\mathbf{q}}_{\mathbf{k},\mathbf{k}+\mathbf{q}}$. (2) For the doped systems, we calculated the Fermi level $\varepsilon_{\rm F}$ and the density of states at the Fermi level $N(\varepsilon_{\rm F})$ with the number of valence electrons reduced using the eigenvalues $\varepsilon_{\mathbf{k}}$ of the non-doped system. (3) By using the results of (1) and (2), we calculated the electron-phonon interaction λ and the other superconducting properties. This approximation is based on the idea that the doping does not greatly change electron and phonon band structures. In this study, we show the results of $0.1 \sim 1.0$ hole-doped systems.

We calculated the superconducting transition temperature by using the Allen-Dynes modified McMillan formula. [18, 19] According to this formula, T_c is given by three parameters: the electron-phonon interaction λ, the logarithmic averaged phonon frequency $\omega_{\log}$, and the screened Coulomb interaction μ^*, in the following form.

$$T_c = \frac{\omega_{\log}}{1.2} \exp\left(\frac{-1.04(1+\lambda)}{\lambda - \mu^*(1+0.62\lambda)}\right). \quad (2)$$

$$\omega_{\log} = \exp\left(\frac{2}{\lambda}\int_0^\infty d\omega \frac{\alpha^2 F(\omega)}{\omega}\log\omega\right). \quad (3)$$

Here, $\alpha^2 F(\omega)$ is the Eliashberg function. λ and $\omega_{\log}$ are obtained by the first-principle calculations using the density functional perturbation theory. [20] As for μ^*, we assume the value $\mu^* = 0.1$. This value holds for weakly correlated materials.

3. Calculation Results and Discussion

First, we optimized the cell parameters. The results show that the optimized structure is delafossite as no structural transition occured. However, the phonon frequency of $CuBO_2$ is negative. It means that the structure is only locally stable. Then after moving some atoms from their initial positions and optimizing the structure again, we found out that $CuBO_2$ relaxed to a body-centered tetragonal structure. This structure is represented by cell parameters a and c, and internal parameter z (Right of Fig. 1). Table 1 shows the optimized cell parameters.

	$CuBO_2$	$CuAlO_2$	$CuGaO_2$	$CuInO_2$
a [Å]	2.534	2.859	3.002	3.367
c/a	4.253	5.965	5.759	5.250
z	0.174	0.110	0.108	0.106

Table 1: The optimized cell parameters of body-centered tetragonal $CuBO_2$ and delafossite $CuAlO_2$, $CuGaO_2$ and $CuInO_2$.

Figures 2 and 3 show the band structures, the densities of states (DOS) and energy gaps. The energy gaps are 1.89 eV for $CuBO_2$, 1.83 for $CuAlO_2$, 0.82 for $CuGaO_2$ and 0.21 for $CuInO_2$. Small gaps of $CuGaO_2$ and $CuInO_2$

show that these covalent bonding is weak. The target materials have the flat valence bands and small peaks of DOS due to the two dimensionality in O-Cu-O dumbbell array. These peaks are mainly constructed by the two-dimensional π-band of Cu $3d_{3z^2-r^2}$-O $2p_z$ anti-bonding states. $CuBO_2$ has wider non-covalent Cu d-band and a narrower peak than $CuAlO_2$. This means that the covalency of $CuBO_2$ is lower than that of $CuAlO_2$ though their energy gaps are the same.

Figure 4 shows the electron-phonon interaction λ. There are peaks at the number of holes $N_h = 0.3$. In $CuBO_2$, a first peak is narrow and a second peak which is due to the narrow DOS peak appears in the heavily doped region of $N_h = 0.7 \sim 1.0$. $CuAlO_2$ has higher λ than $CuBO_2$, $CuGaO_2$ and $CuInO_2$. The difference in λ strength is due to the covalency mentioned above.

Figure 5 shows the logarithmic averaged phonon frequency ω_{log}. These are almost constant for the number of holes. The difference of ω_{log} is mainly due to atomic mass. Therefore, $CuGaO_2$ and $CuInO_2$ have smaller ω_{log} than $CuBO_2$ and $CuAlO_2$. In the lightly doped region, $CuBO_2$ and $CuAlO_2$ have almost the same ω_{log} though Al is heavier than B. This is due to large electron-phonon interaction of $CuAlO_2$.

Figure 6 shows the superconducting transition temperature T_c. Since $CuInO_2$ has very low T_c ($< 1\,K$), its curve is no longer invisible in Fig. 6. The T_c variation is determined mainly by the electron-phonon interaction because logarithmic averaged phonon frequencies ω_{log} are almost constant for the number of holes. $CuBO_2$, $CuGaO_2$ and $CuInO_2$ have much lower T_c than $CuAlO_2$ because they have low covalency and λ as mentioned above.

4. Conclusions

In summary, we calculated the chemical trend of superconducting transition temperature of the hole-doped delafossite $CuBO_2$, $CuAlO_2$, $CuGaO_2$ and $CuInO_2$. The calculated T_c are about 50 K for $CuAlO_2$, 10 K for $CuBO_2$ and $CuGaO_2$ and 1 K for $CuInO_2$ at maximum in the optimum hole-doping concentration. The low T_c of $CuInO_2$ is attributed to the weak electron-phonon interaction caused by the low covalency and heavy atomic mass.

Acknowledgment

The authors acknowledge the financial support from the Global Center of Excellence (COE) program "Core Research and Engineering of Advanced

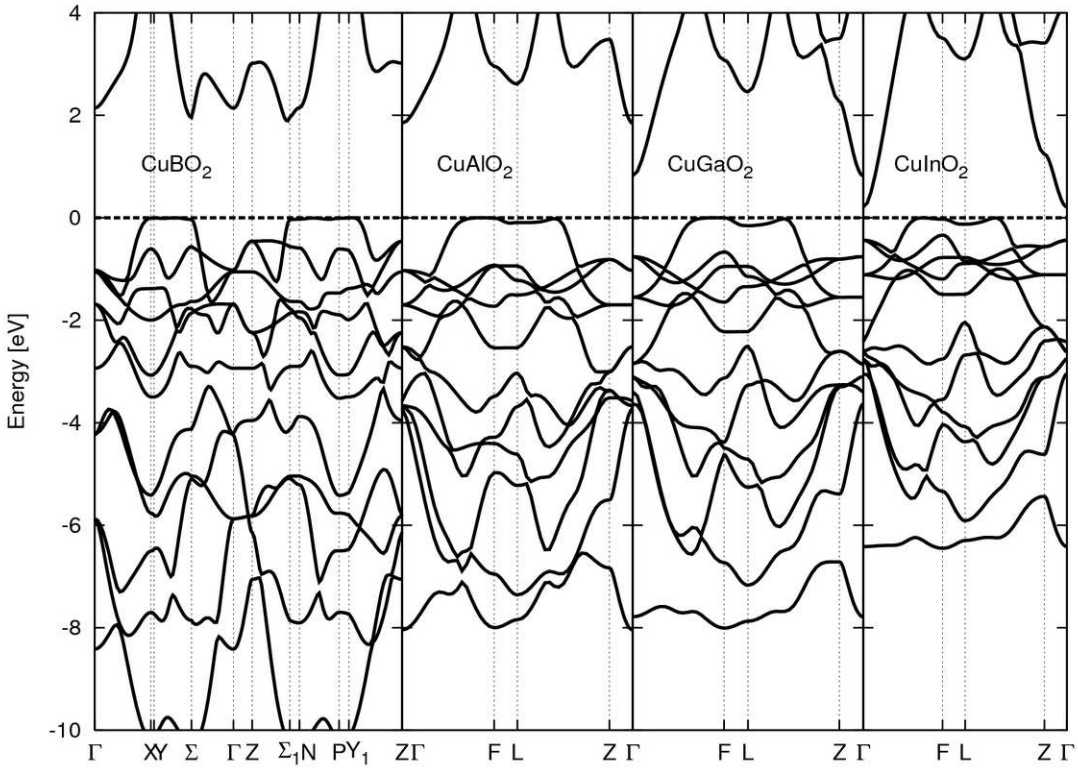

Figure 2: Band structures of $CuBO_2$, $CuAlO_2$, $CuGaO_2$ and $CuInO_2$.

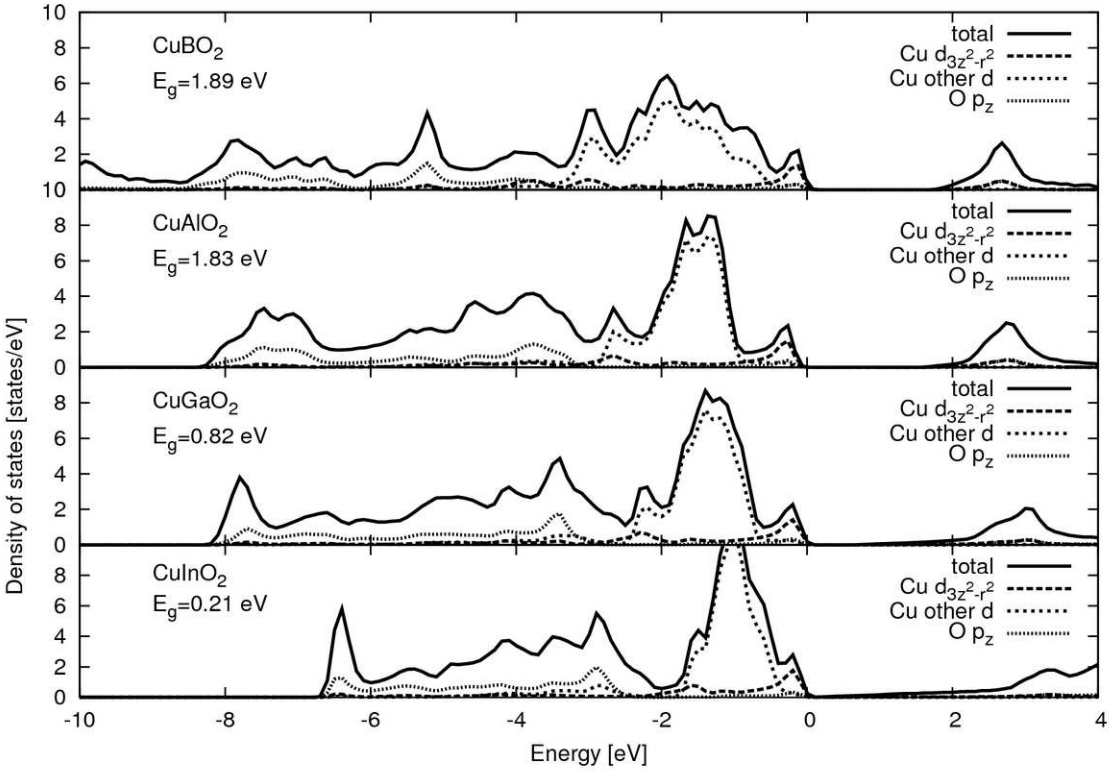

Figure 3: Density of states and energy gaps.

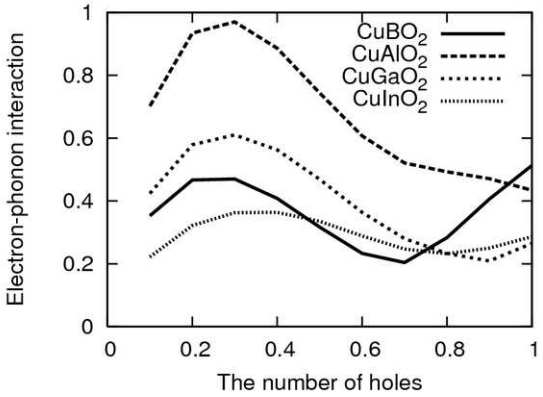

Figure 4: Electron-phonon interaction λ.

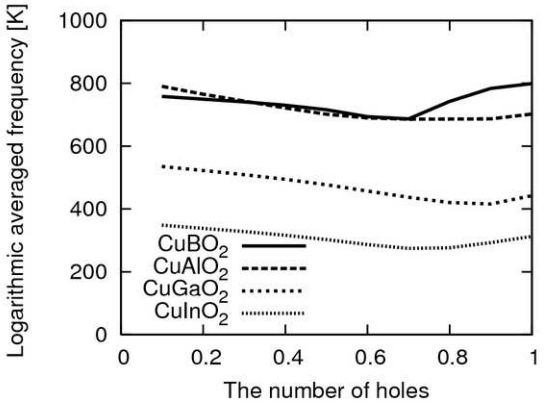

Figure 5: Logarithmic averaged phonon frequency $\omega_{\log}$.

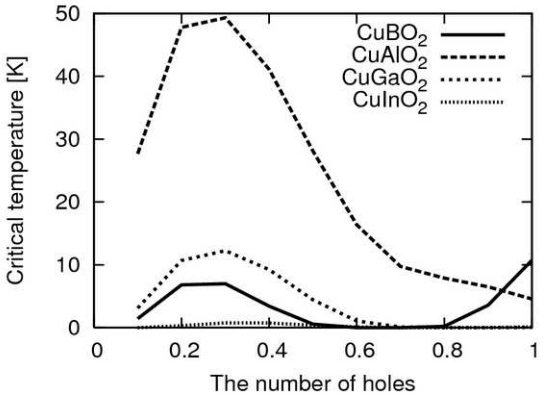

Figure 6: Superconducting transition temperature $T_{\rm c}$.

Materials - Interdisciplinary Education Center for Materials Science", the Ministry of Education, Culture, Sports, Science and Technology, Japan, and a Grant-in-Aid for Scientific Research on Innovative Areas "Materials Design through Computics: Correlation and Non-Equilibrium Dynamics". We also thank to the financial support from the Advanced Low Carbon Technology Research and Development Program, the Japan Science and Technology Agency for the financial support.

References

[1] H. Kawazoe, M. Yasukawa, H. Hyodo, M. Kurita, H. Yanagi, H. Hosono, Nature 389 (1997) 939.

[2] A. Nakanishi, H. Katayama-Yoshida, J. Phys. Soc. Jpn. 80 (2011) 024706.

[3] A. Nakanishi, H. Katayama-Yoshida, J. Phys. Soc. Jpn. 80 (2011) 053706.

[4] H. Funashima, A. Yanase, H. Harima, H. Katayama-Yoshida, Proceedings of 23rd International Conference on Thermoelectrics (2004) 237–238.

[5] H. Katayama-Yoshida, H. Funashima, I. Hamada, H. Harima, A. Yanase, Fabrication method and high-efficient thermo-electric power materials by two-dimensional natural super-lattices of $cualo_2$, Japan Patent 652696 (2009).

[6] I. Hamada, H. Katayama-Yoshida, Physica B 376 (2006) 808.

[7] H. Katayama-Yoshida, T. Koyanagi, H. Funashima, H. Harima, A. Yanase, Solid State Communication 126 (2003) 135.

[8] A. Nakanishi, H. Katayama-Yoshida, Solid State Communication 152 (2012) 24.

[9] A. Nakanishi, H. Katayama-Yoshida, Solid State Communication 152 (2012) 2078–2081.

[10] P. Hohenberg, W. Kohn, Phys. Rev. 136 (1964) B864.

[11] W. Kohn, L. J. Sham, Phys. Rev. 140 (1965) A1133.

[12] P. Giannozzi, S. Baroni, N. Bonini, M. Calandra, R. Car, C. Cavazzoni, D. Ceresoli, G. L. Chiarotti, M. Cococcioni, I. Dabo, A. D. Corso, S. Fabris, G. Fratesi, S. de Gironcoli, R. Gebauer, U. Gerstmann, C. Gougoussis, A. Kokalj, M. Lazzeri, L. Martin-Samos, N. Marzari, F. Mauri, R. Mazzarello, S. Paolini, A. Pasquarello, L. Paulatto, C. Sbraccia, S. Scandolo, G. Sclauzero, A. P. Seitsonen, A. Smogunov, P. Umari, R. M. Wentzcovitch, J. Phys.:Condens. Matter 21 (2009) 395502.

[13] Phys. Rev. B 46 (1992) 6671.

[14] J. P. Perdew, K. Burke, M. Ernzerhof, Phys. Rev. Lett. 77 (1996) 3865.

[15] D. Vanderbilt, Phys. Rev. B 41 (1990) 7892.

[16] H. J. Monkhorst, J. D. Pack, Phys. Rev. B 13 (1976) 5188.

[17] M. Parrinello, A. Rahman, Phys. Rev. Lett. 45 (1980) 1196.

[18] W. L. McMillan, Phys. Rev. 167 (1968) 331.

[19] P. B. Allen, R. C. Dynes, Phys. Rev. B 12 (1975) 905.

[20] S. Baroni, S. de Gironcoli, A. D. Corso, P. Giannozzi, Rev. Mod. Phys. 731 (2001) 515.